

Review

# Microcoil nuclear magnetic resonance spectroscopy

A.G. Webb\*

*Department of Electrical and Computer Engineering, and Beckman Institute for Advanced Science and Technology, University of Illinois at Urbana-Champaign, 4221 Beckman Institute, 405 N. Mathews, Urbana, IL 61801, USA*

Received 1 September 2004; received in revised form 15 January 2005; accepted 22 January 2005

Available online 28 April 2005

## Abstract

In comparison with most analytical chemistry techniques, nuclear magnetic resonance has an intrinsically low sensitivity, and many potential applications are therefore precluded by the limited available quantity of certain types of sample. In recent years, there has been a trend, both commercial and academic, towards miniaturization of the receiver coil in order to increase the mass sensitivity of NMR measurements. These small coils have also proved very useful in coupling NMR detection with commonly used microseparation techniques. A further development enabled by small detectors is parallel data acquisition from many samples simultaneously, made possible by incorporating multiple receiver coils into a single NMR probehead. This review article summarizes recent developments and applications of “microcoil” NMR spectroscopy. © 2005 Elsevier B.V. All rights reserved.

*Keywords:* Limits of detection; Microcoils; Limited sample mass; Miniaturization; Parallel data acquisition

## Contents

1. Introduction .....	892
2. Intrinsic NMR sensitivity .....	893
3. Development of small coils for high-resolution NMR .....	894
4. Sensitivity comparisons .....	895
5. Small coil applications of proton NMR spectroscopy .....	895
6. Protein applications .....	896
7. Multiple coil probeheads .....	898
8. Hyphenation of microseparation techniques with NMR detection .....	900
9. Other applications of small coils .....	900
10. Conclusion .....	901
Acknowledgements .....	901
References .....	902

## 1. Introduction

Nuclear magnetic resonance (NMR) spectroscopy is one of the most widely used and versatile analytical techniques, applicable to gaseous, liquid and solid samples, and can be

used to study chemical structure, molecular dynamics and binding kinetics. Many potentially interesting scientific studies, however, cannot be performed using NMR due to the inherent low sensitivity of the technique. In particular, when the mass of a particular sample is limited, the data acquisition times required to obtain useful spectra can become unreal-

\* Tel.: +1 217 333 7480; fax: +1 217 244 0105.  
E-mail address: [agwebb@uiuc.edu](mailto:agwebb@uiuc.edu).

istically long. Such situations include structural analyses of the products of combinatorial and multi-stage chemical syntheses, extracts from rare plants with pharmacological properties, and certain “metabonomic” samples. The low sensitivity also precludes many studies of dynamic processes on short time-scales. Efforts to improve the sensitivity of NMR have included a continuous increase in the strength of static magnetic fields [1], the development of cryogenically cooled detectors [2] (covered in detail later in this paper), and the use of hyperpolarisation techniques [3,4]. This paper concentrates on an approach using very small, highly sensitive radio frequency (RF) detectors. As will be discussed later, the strategy required to maximize the signal-to-noise (S/N) of the NMR measurement is to dissolve the sample of interest at its maximum concentration in the minimum amount of solvent, and then to use the smallest RF coil which encompasses this volume. Although simple in concept, this approach presents many challenges, including the optimization of static magnetic field ( $B_0$ ) and radio frequency field ( $B_1$ ) homogeneity, the physical introduction of small sample volumes into the detector, and the tuning of the coil to multiple frequencies for heteronuclear experiments.

Commercial and academic enterprises have both been active in recent years in producing coils which have active volumes in the low microliter to low nanoliter range. In addition to their high sensitivity, small coils have several other advantages and interesting properties. For example, signals from solvent impurities are much less prominent with decreasing sample volume. For electrically conductive samples, such as “biological” solutions which contain a substantial salt component, there is also a reduction of the loading effects of the sample. Another advantage of small-volume probes is that the amount of deuterated solvents can be dramatically reduced for NMR coupled separations. Small coils have also been reported to be extremely simple to shim [5]. Finally, small coils allow the design of probeheads containing more than one coil, enabling a range of new types of NMR experiments to be performed.

## 2. Intrinsic NMR sensitivity

The limit of detection (LOD) of a particular measurement method is defined, either in terms of concentration or mass LOD, as the smallest measure that can be detected “with reasonable certainty” [6]. Mathematically:

$$x_L = x_b + k\sigma_b \quad (1)$$

where  $x_L$  is the aforementioned smallest measure,  $x_b$  the mean of blank measurements,  $\sigma_b$  the standard deviation of the blank measurements and  $k$  is a numerical factor which determines the confidence level. IUPAC suggests a value of  $k=3$  [7], corresponding to a confidence level of  $\sim 90\%$ . In comparison with many other analytical techniques, NMR suffers from poor limits of detection. For example, laser in-

duced fluorescence (LIF) can detect concentrations as low as 100 fM, Fourier-transform ion cyclotron resonance (FTICR) tens of zeptomoles of material, Fourier-transform infrared spectroscopy has LODs as low as  $10^{-12}$  to  $10^{-15}$  mol as does Raman spectroscopy, and mass spectrometry has achieved  $10^{-19}$  mol, but LODs for NMR are several orders of magnitude poorer. The NMR signal depends upon the net magnetization,  $M_0$ , of the sample. As a simple example, if a two-level system with spin quantum number,  $I$ , equal to  $1/2$  is considered, then:

$$M_0 = \frac{\gamma h}{4\pi} (N_{\text{parallel}} - N_{\text{anti-parallel}}) = \frac{\gamma^2 h^2 B_0 N_s}{16\pi^2 kT} \quad (2)$$

where  $\gamma$  is the gyromagnetic ratio of the nucleus,  $h$  the Planck’s constant,  $N_{\text{parallel}} - N_{\text{anti-parallel}}$  the difference in populations between the two energy levels,  $B_0$  the static magnetic field,  $N_s$  the total number of nuclei in the sample,  $k$  the Boltzmann’s constant and  $T$  is the temperature. For protons at a static magnetic field of 11.7 T there is only a factor of  $5 \times 10^{-6}$  difference in the populations of the parallel and anti-parallel states, and this very small value is the reason for the intrinsic low sensitivity of NMR as a measurement technique. The problem becomes even more pronounced if protons are not the nuclei being detected, but a nucleus such as  $^{13}\text{C}$  which has small gyromagnetic ratio, roughly one-quarter that of protons, and a low natural abundance, 1.1%.

In order to determine the S/N of the NMR measurement, the properties of the NMR detector and total measurement system must be included. The S/N can be expressed as [8]:

$$\frac{S}{N} \propto \frac{k_0(B_1/i)V_s N \gamma (h^2/4\pi^2) I(I+1) (\omega_0^2/kT 3\sqrt{2})}{\sqrt{4kT \Delta f (R_{\text{coil}} + R_{\text{sample}})}} \quad (3)$$

where  $V_s$  is the sample volume,  $k_0$  a constant which accounts for spatial inhomogeneities in the  $B_1$  field produced by the probe,  $N$  the spin density,  $\omega_0$  the Larmor frequency,  $\Delta f$  is the measurement bandwidth,  $R_{\text{coil}}$  and  $R_{\text{sample}}$  are the coil and sample resistances, respectively, and the factor of  $\sqrt{2}$  is introduced since the noise measure is root-mean-square (rms). The factor  $B_1/i$ , the magnetic field per unit current, is defined to be the coil sensitivity.

If the S/N of a particular measurement is too low to be useful, then the only method to increase the S/N for a given experimental setup is to repeat the measurement a number of times and co-add the results: since the signal between scans is coherent, and the noise is incoherent, the S/N increases by a factor proportional to the square root of the number of co-added measurements. However, this is clearly a very time-consuming operation with, for example, a 10-fold improvement in S/N requiring a 100-fold increase in experiment time.

Eq. (3) suggests a number of avenues to maximize the S/N of an NMR experiment. The first is to use as high a static magnetic field as possible: currently, 21.1 T (proton Larmor frequency 900 MHz) is the highest field available for high-resolution NMR studies, although reports exist at 24.7 T for an experimental magnet [9] and pulsed field magnets have

been used for initial NMR results at 58 T [10]. The second option is to reduce the noise voltage from the NMR coil via the use of superconducting materials: this has resulted in the development of “cryoprobes” from all of the major NMR manufacturers [2,11–16]. Typical S/N increases of a factor of 4–5 are possible for samples with low conductivity using this technology, with these factors becoming lower as the sample conductivity increases. The third possibility is to increase the intrinsic sensitivity of the coil. As shown by Hault and Richards [8], the value of  $B_1/i$  for both saddle and solenoid coil geometries is inversely proportional to the diameter of the coil. Further analysis by Peck et al. [17] showed that, for very small solenoids, this relationship holds for coil diameters as low as  $\sim 100 \mu\text{m}$ , below which the sensitivity increases proportional to the square root of the coil diameter. It is clear, then, that the maximum sensitivity can be realized by making the coil as physically small as possible to accommodate the sample. The volume of the sample should be its minimum value, corresponding to the highest possible concentration of solute.

### 3. Development of small coils for high-resolution NMR

As mentioned previously, much recent activity, both commercially and academically, has focused on the design of small coils for NMR spectroscopy. Three basic geometries have been used, namely saddle, solenoidal and planar. The particular advantages of the vertical saddle geometry are re-

lated to easy sample placement using conventional rotors and thin, vertically oriented NMR sample tubes. The earliest work demonstrating the potential of small-coil high-resolution NMR spectroscopy was performed by Shoolery [18], who published a number of applications for both  $^1\text{H}$  and  $^{13}\text{C}$  using a 1.7 mm diameter saddle coil at relatively low magnetic fields. The development of 3 and 2.5 mm micro-NMR probes with sample volumes of 150 and 100  $\mu\text{L}$ , respectively, at 11.7 T was reported by Bruker in 1992 [19]. In 1998, Nalorac developed a 1.7-mm submicroprobe with a 30  $\mu\text{L}$  fill volume: a comparison with previous 3 mm diameter probes showed the expected gains in S/N [20]. Bruker (Switzerland) developed a 2.5  $\mu\text{L}$  active volume triple resonance/X-nucleus/inverse detection (TXI) probe in 2002 [21].

In 1993, a magic angle spinning liquid nano-NMR probe (Varian) with 40  $\mu\text{L}$  sample volume was introduced [22,23], based on a 4 mm diameter solenoid coil oriented at the magic angle with respect to  $B_0$ . Developing a number of academic ideas using small solenoid coils surrounded by a perfluorinated fluid for susceptibility matching [24–29], in 2000 Protasis/MRM produced a 1.5  $\mu\text{L}$  active volume solenoid-based probe, which has been used extensively for hyphenation to capillary separations [30]. The main advantage of solenoid coils is the higher sensitivity compared to saddle coils: depending upon the length-to-diameter ratio of the coils the solenoid has between a factor of two and three higher sensitivity, translating directly into a higher S/N. Extensive analyses of various aspects of solenoid coils have been published [31–36]: photographs of small solenoids are shown in Fig. 1(a). The major disadvantage of the geometry is that

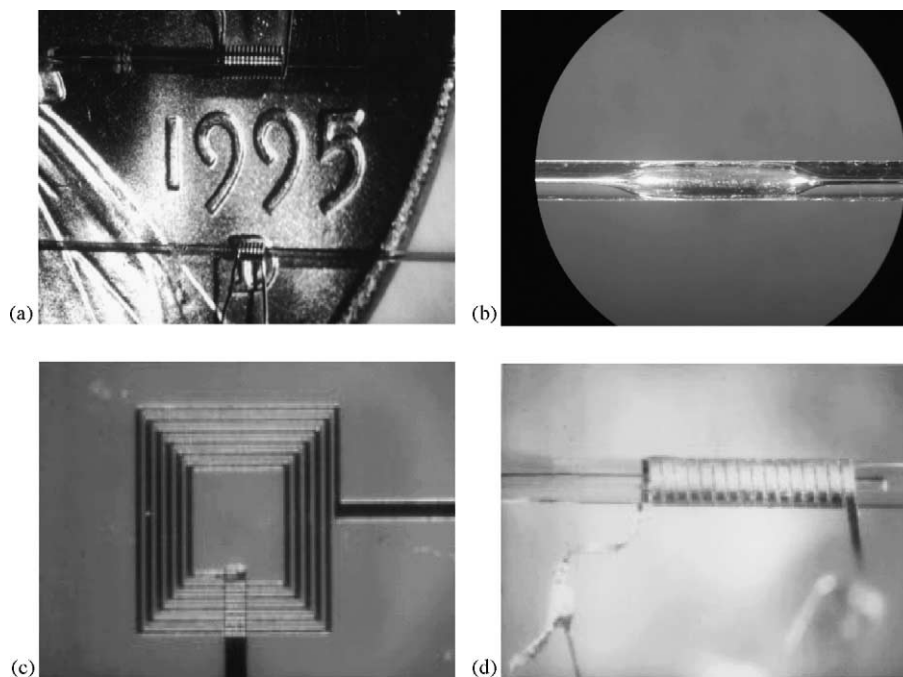


Fig. 1. (a) Two hand-wound solenoidal coils with outer diameters 350 and 150  $\mu\text{m}$ . (b) Hydrogen fluoride etched bubble cell to increase the filling factor for NMR coupled separations. (c) Micromachined square surface coil detector with inner diameter 60  $\mu\text{m}$ . (d) Micropatterned solenoidal coil. (d) is reproduced from Ref. [38], © 1997 with permission from the American Institute of Physics.

sample loading is now quite involved. Most solenoid coils use some form of flow sample injection, which is generally considered to be less convenient than the use of discrete sample tubes. In such flow-through probes, there is often a need to increase the filling factor of such probes by using a bubble cell. Formation of such a bubble cell can be achieved using, for example, hydrofluoric acid etching: an example is shown in Fig. 1(b).

A number of reports have used various microfabrication techniques to construct detectors for small-volume NMR spectroscopy [37–45]. Most of the geometries have been planar, as shown in Fig. 1(c), although saddle [43] and solenoid [38] geometries, the latter shown in Fig. 1(d), have also been produced. In all of these cases, the quality of the spectra, both in terms of linewidth and sensitivity, has not been as good as obtained using the more labour-intensive hand-wound coils. Nevertheless, microfabrication is a promising area particularly in terms of parallel data acquisition and the integration of NMR detection with microfluidics.

#### 4. Sensitivity comparisons

NMR sensitivity can be defined in terms of mass sensitivity,  $S_m$ , or concentration sensitivity,  $S_c$ , as discussed in detail elsewhere [46]. Simple equations, with relevant units, are given below:

$$S_c = \frac{S/N}{C} (\mu\text{M}^{-1}), \quad S_m = \frac{S/N}{m} (\text{ng}^{-1}) \quad (4)$$

The  $S/N$  per unit mass increases as the size of the coil decreases, and therefore in situations where the mass of the sample is limited, and high concentrations are possible to prepare, the  $S/N$  achieved with a small coil is higher than using a larger coil. In the case that only low concentrations are possible, due either to solubility constraints or biological activity in proteins, and the total mass is not limited, then larger coils give a higher  $S/N$ . In the intermediate regime, where mass and concentration are both limited, then the optimum size of the coil is dictated by the relative values of these two variables.

A number of studies have been performed comparing the sensitivity of recently developed small coils with standard larger coils. In one such study by Schlotterbeck et al. [21], the mass sensitivity of the Bruker 1-mm TXI microliter probe with a sample in a 1 mm diameter capillary tube was shown to be five times greater than a 5-mm conventional TXI probe: the sample used was sucrose in aqueous solution at 600 MHz. The small TXI probe also showed a factor of 1.7 enhancement over a 5-mm TXI cryoprobe with the sample in a 5 mm tube, and a factor of 1.3 over a 5-mm TXI cryoprobe with the sample contained in a 1 mm capillary.

A second detailed sensitivity analysis of different probes at 600 MHz was published by Olson et al. [46]. Although some data had to be inferred from the literature, the general results show that the 1.5  $\mu\text{L}$  CapNMR probe and 5-mm cry-

oprobe have very similar mass sensitivities, and that these are approximately 10 times greater than the mass sensitivity of a standard 5-mm probe. The concentration sensitivity of the CapNMR probe was found to be approximately 15 times poorer than the 5-mm probe.

#### 5. Small coil applications of proton NMR spectroscopy

Given previous discussions, it is clear that small-volume probes are ideally suited to situations where the total sample mass is limited, but the sample is relatively soluble in the relevant solvent. Three applications in the areas of combinatorial chemistry analysis [47], plant extracts [48] and metabolic profiling of *in vivo* samples from animal models [49] are summarized here.

In the first application [47], a solenoidal NMR microprobe with an observe volume of 800 nL was used to acquire high-resolution  $^1\text{H}$  NMR spectra from the cleaved product of individual 160- $\mu\text{m}$  diameter Tentagel beads, which are often used in solid-phase synthesis for combinatorial chemistry. This work focused on one compound discovered in a series of serine protease inhibitors [50] with leukotriene B4 receptor binding affinity. The cleaved product was dissolved in dimethylsulphoxide and sandwiched between two perfluorinated organic liquid plugs. NMR spectra of the product cleaved from single beads were acquired at 600 MHz in  $\sim 1$  h. Carr–Purcell–Meiboom–Gill (CPMG) experiments were performed to remove broad baseline components in the spectrum. Representative spectra are shown in Fig. 2. Based on calibration experiments, the total amount of material cleaved from a single bead was estimated to be  $540 \pm 170$  pmol, with approximately 180 pmol within the observe volume of the probe.

The second example illustrates the utility of small flow-through probes for high throughput analysis of small amounts of sample. Eldridge et al. [49] used a Protasis/MRM 5  $\mu\text{L}$  indirect carbon gradient flow probe with an active volume of 1.5  $\mu\text{L}$  in the analysis of a large natural product library. The particular illustrative compound was an extract of *Taxus brevifolia*, the pacific yew tree, containing paclitaxel (Taxol) and its derivatives. Five to ten micrograms of material was sufficient for 2D COSY experiments, with  $\sim 50$   $\mu\text{g}$  needed for experiments such as gradient HMQC and HMBC. Fig. 3 shows a  $^1\text{H}$  spectrum of paclitaxel which, in combination with the COSY data, allowed the identification of major peaks from a series of related compounds.

In the final example, a Bruker 1 mm TXI probe with an active volume of 2.5  $\mu\text{L}$  was used for metabolic profiling of rodent biological fluids [43]. Since only  $\sim 2$   $\mu\text{L}$  of fluid is needed for this probe, this volume could be removed from the animals without the need for euthanasia, unlike the case for the larger volumes needed for larger probes. Fig. 4 shows results, together with spectral assignments, obtained at 600 MHz.

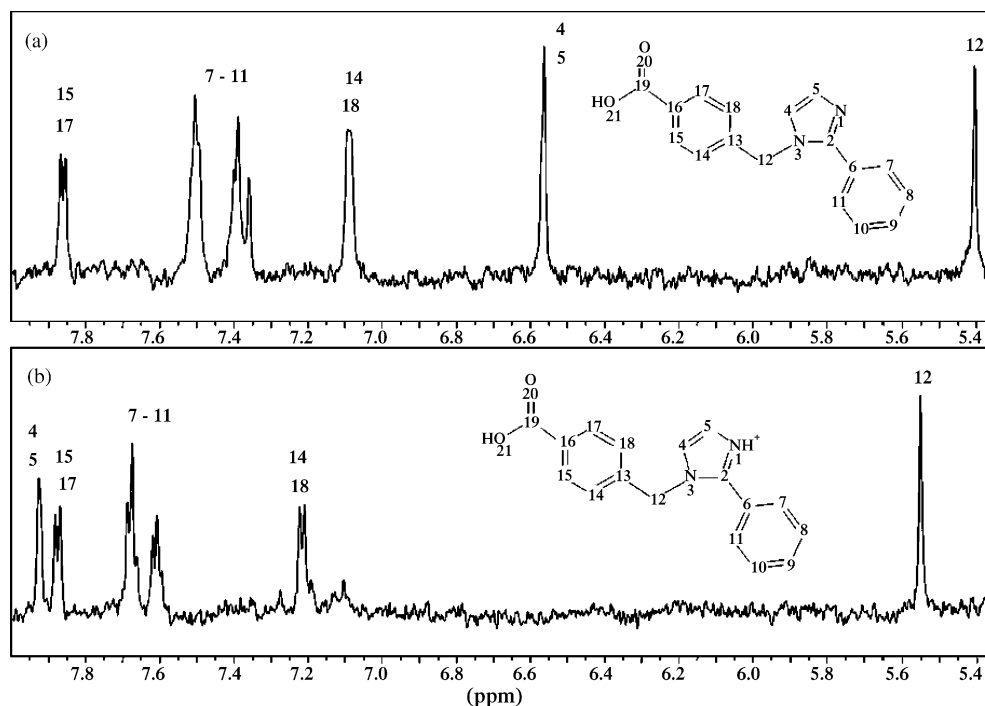


Fig. 2. The  $^1\text{H}$  CPMG spectra obtained from the cleaved product of a single bead: (a) dissolved in neat  $\text{DMSO-}d_6$  and (b) dissolved in acidified  $\text{DMSO-}d_6$ . Figure reproduced from Ref. [47], © 2001 with permission from Elsevier.

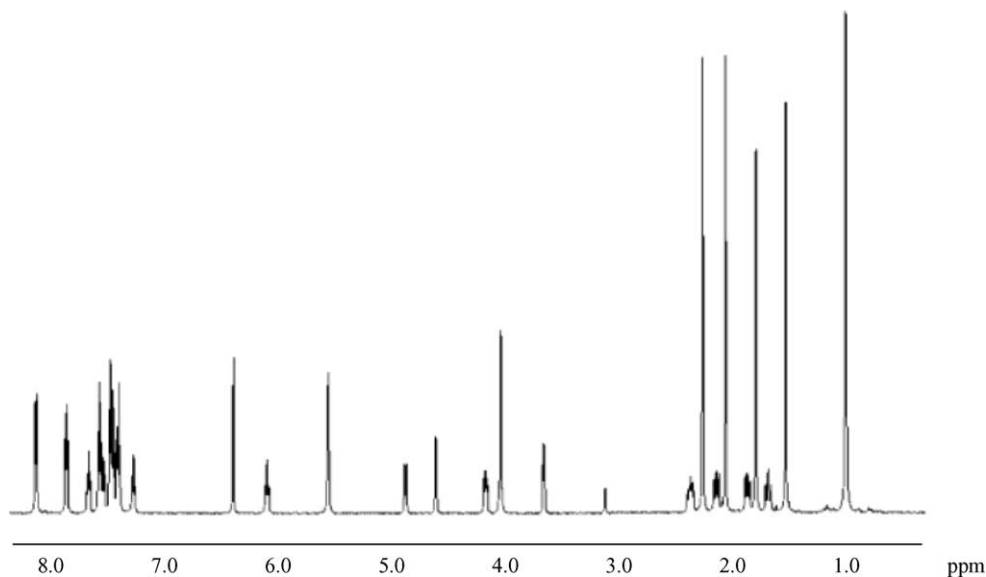


Fig. 3.  $^1\text{H}$  NMR spectrum of 50  $\mu\text{g}$  of paclitaxel in 3  $\mu\text{L}$   $\text{CD}_3\text{OD}$  acquired using a 5- $\mu\text{L}$  microcoil flow probe at 600 MHz. Reproduced with permission from Ref. [49], © 2002 American Chemical Society.

## 6. Protein applications

NMR studies involving proteins require probes, which operate at a number of different frequencies. For standard heteronuclear experiments TXI probes allow pulsing on proton, deuterium, carbon and nitrogen channels. The usual configuration for saddle coils contains two RF coils, each tuned to two frequencies, whereas solenoidal-based probes

typically have only one coil, which is tuned to all four frequencies.

Recently, small coils have been developed for protein experiments. The use of small solenoidal coils allows reduced amounts of protein to be used: this facet is likely to be particularly important in the case of proteins produced in eukaryotic cells rather than bacteria, where isotopic enrichment is considerably more difficult and expensive. The electrical circuit



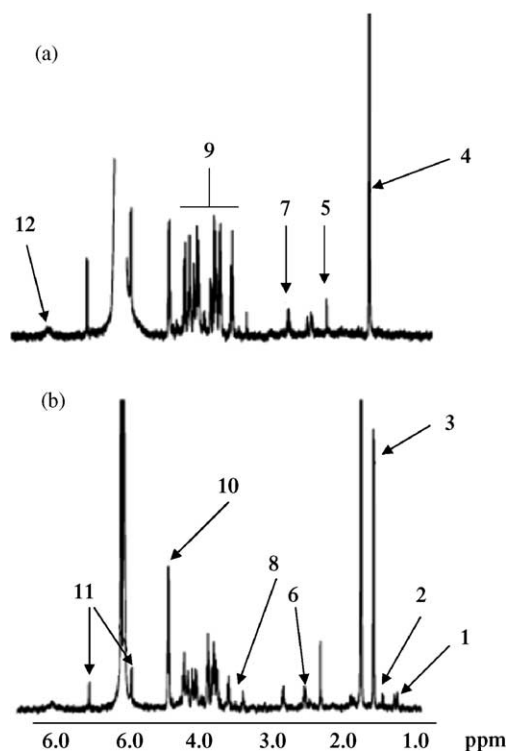


Fig. 4. 600 MHz  $^1\text{H}$  NMR spectra of rat (a) and mouse (b) cerebrospinal fluid (CSF) using a microliter probe with 128 scans. Both spectra were acquired using a water presaturation sequence based on the start of the NOESY pulse sequence. Two milliliters of CSF were diluted with 3 mL of  $\text{D}_2\text{O}$ . Key: (1) leucine + valine; (2) valine; (3) propandiol (vehicle for anaesthetic); (4) lactate; (5) acetate; (6) glutamine; (7) glutamine; (8) creatine; (9) glucose; (10) lactate; (11) H1 glucose; (12) amino groups. Reproduced from Ref. [48], with permission of The Royal Society of Chemistry.

used in a 2.5 mm diameter, solenoid TXI probe [51] is shown in Fig. 5. The L1–C1 trap presents a very low impedance at low frequency and high impedance at high frequency. The L2–C6–C7 tank circuit appears as a high impedance at the proton frequency, but as a very low impedance path at the  $^{15}\text{N}$  frequency. The proton channel has the shortest electrical path to the sample coil in order to minimize signal loss. L–C trap circuits at both  $^{15}\text{N}$  and  $^{13}\text{C}$  frequencies are used between the  $^{15}\text{N}$  and  $^{13}\text{C}$  channels, and the lock channel is attached to the  $^{13}\text{C}$  channel with a trap circuit at the  $^{13}\text{C}$  frequency.

In Ref. [51], the  $90^\circ$  pulse widths for all channels were compared with those from a commercial 5 mm TXI probe: the values were  $4.0\ \mu\text{s}$  versus  $12\ \mu\text{s}$  ( $^1\text{H}$ , 50 W amplifier, 6 dB attenuation),  $3.8\ \mu\text{s}$  versus  $43\ \mu\text{s}$  ( $^{15}\text{N}$ , 300 W amplifier, full power) and  $1.8\ \mu\text{s}$  versus  $14\ \mu\text{s}$  ( $^{13}\text{C}$ , 300 W amplifier, full power). The much shorter  $^{13}\text{C}$  pulses are particularly important for experiments at high  $B_0$  fields since they allow a much higher excitation bandwidth. Fig. 5 shows specific two-dimensional  $^1\text{H}$ ,  $^{15}\text{N}$  planes extracted at different  $^{13}\text{C}=\text{O}$  frequencies from a three-dimensional HNCO spectrum collected on a 1 mM, double-labeled  $^{15}\text{N}/^{13}\text{C}$  IA-3 sample using the TXI solenoidal probe. IA-3 is an intrinsically unstructured 68 amino acid protein inhibitor of yeast proteinase A [52].

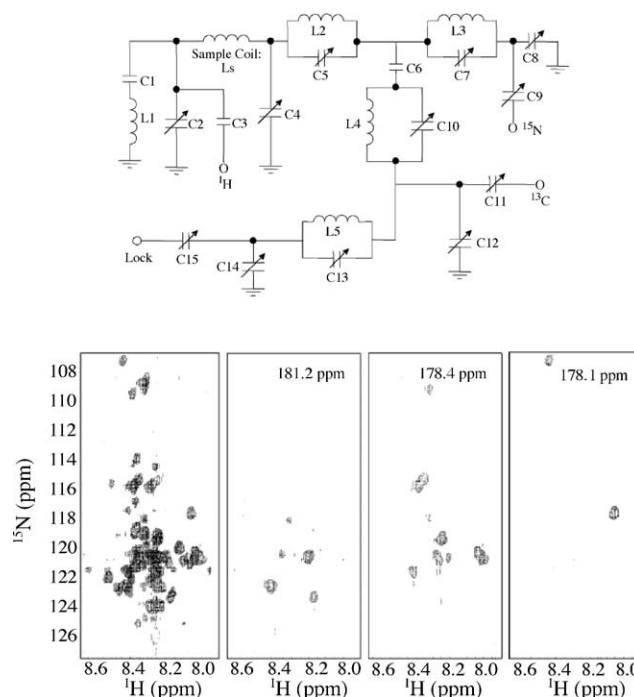


Fig. 5. (Top) Circuit diagram for the TXI solenoidal probe used to acquire the 3D HNCO data (bottom) of double-labeled 1 mM  $^{15}\text{N}/^{13}\text{C}$  IA-3 using a triple-resonance solenoidal probe. Experimental parameters: sw 6614 Hz, sw1 ( $^{15}\text{N}$ ) 1302 Hz, sw2 ( $^{13}\text{C}$ ) 3001 Hz, 32 signal averages, 64 real data points in the  $^{13}\text{C}=\text{O}$  dimension, 60 real data points in the  $^{15}\text{N}$  dimension, 4096 complex acquisition data points, total data acquisition time 59 h. Solvent suppression used presaturation. The 2D projection of all the  $^{13}\text{C}=\text{O}$  frequencies is shown in the leftmost panel, and the plots of selected single  $^{13}\text{C}=\text{O}$  slices are shown in the other three panels. Figure reproduced from Ref. [51], © 2003 with permission from Elsevier.

A second protein study [5] used a commercial microcoil probe from Protasis/MRM. The volume of the TXI HCN z-gradient microcoil NMR probe is  $5\ \mu\text{L}$  with an active volume of  $1.5\ \mu\text{L}$ . Most of the experiments were performed using proteins from the *Thermotoga maritima* proteome [53], in particular, the conserved hypothetical protein, TM0979. HNCA/HNCOCA spectra were acquired to test the ability to perform the sequential backbone assignment of TM0979. In the HNCA spectrum, all inter- and intrasidue peaks were detectable, nearly all  $\text{C}_\alpha$  and  $\text{C}_\beta$  peaks were observed in the CBCACONH spectrum, and all CO correlation peaks could be identified from the HNCO spectrum, allowing complete backbone assignment of TM0979.

As outlined previously, the very short  $^{13}\text{C}$  pulse widths are particularly important in a number of pulse sequences: in this particular study, it was possible to record a single HCCH–TOCSY spectrum [54,55] across the full aliphatic and aromatic side-chain carbon range. This experiment allows complete side-chain assignment of all amino acids in a protein within a single spectrum. The correlation between the aliphatic and aromatic carbons is hindered due to the large carbon chemical shift ranges (aliphatic carbons, 0–75 ppm; aromatic carbons, 115–140 ppm) which corresponds to a

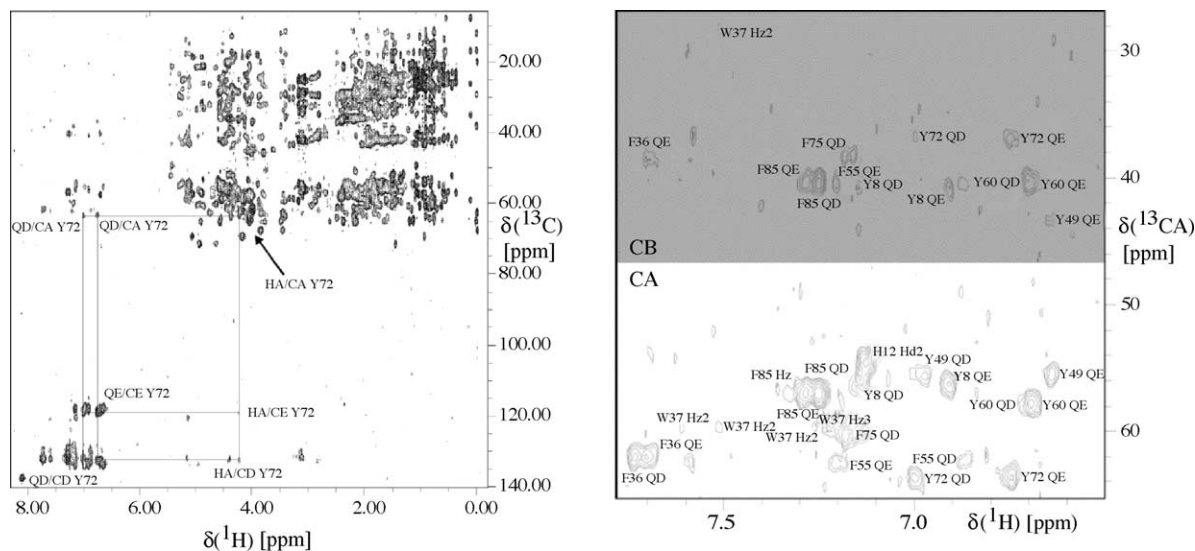


Fig. 6. (Left) 2D [ $^1\text{H}$ ,  $^{13}\text{C}$ ] aliphatic–aromatic HCCH–TOCSY FLOPSY-16 spectrum recorded with a mixing time of  $\tau_m = 11.77$  ms. The assignment of tyrosine 72 based on the  $\text{C}_\alpha$  chemical shift is indicated in the spectrum (10 mM  $^{13}\text{C}/^{15}\text{N}$  TM0979, 313 K, measurement time 30 h). (Right) Enlargement of the  $\text{C}_\alpha/\text{C}_\beta$  carbon chemical shift–proton aromatic chemical shift region. All cross-peaks are annotated, and the complete aromatic chemical shift assignment can be achieved. The  $\text{C}_\beta$  cross-peak area is highlighted with a gray box. Reproduced with permission from Ref. [5], © 2004 American Chemical Society.

bandwidth of roughly 20 kHz at 14.1 T. Standard 5 mm NMR probes or cryoprobes are not rated for the high power levels required to produce Hartman–Hahn mixing over this broad chemical shift range. An HCCH–TOCSY spectrum with a  $z$ -filter FLOPSY-16 mixing sequence using a 20 kHz spin lock field was used to acquire the spectra shown in Fig. 6. This type of spectrum can be used for the assignment of connectivities between the aliphatic  $\text{C}_\alpha$  and  $\text{C}_\beta$  atoms and the rest of the aromatic side chain, and also within the aromatic ring itself, in one measurement, thus accelerating greatly aromatic side-chain assignment.

## 7. Multiple coil probeheads

The small size of a microcoil, compared to the extent of homogeneous  $B_0$  field within the bore of a standard NMR magnet, enables multiple coils to be incorporated into a single probehead. The technical challenges in producing a practical multi-coil probe include maintaining high local  $B_0$  homogeneity for each sample despite the presence of the other coils, achieving maximum sensitivity for each coil, and separating the signals from each sample either through hardware or software. Applications of multi-coil technology include increasing the throughput of NMR by acquiring data from more than one sample simultaneously [56–63], as well as enabling other specialized types of experiment such as removing line-broadening effects in NMR-detected electrophoretic separations [64], monitoring rapid chemical reactions [65] and performing solvent suppression [66].

Two basic approaches have been used in designing probeheads with multiple coils. In the first, the coils are connected

in parallel [58,59,61,66], effectively forming a single resonant circuit, and the signals from each sample are separated through the use of spatially selective pulse sequences. The alternative approach is to construct a number of separate RF circuits, one for each coil [55,57,60,63–65], and then either to use multiple receiver channels or time-domain multiplex the signals into a single receiver, in order to separate the signals from each coil.

The most promising application of increasing NMR throughput is in the area of screening large compound libraries with target protein molecules [67–70]. In terms of increasing NMR throughput, the maximum number of coils that have been incorporated into a single probehead is currently eight [63], with each coil having an observation volume of  $\sim 35$  nL. In this probehead, Teflon flow tubes were attached to both ends of the capillary for sample loading. The coils were mounted one above the other with a vertical spacing of approximately 3 mm and alternate coils were rotated  $90^\circ$  with respect to each other to minimize the coupling. Using a vertical separation smaller than 3 mm resulted in substantial distortions of the local static magnetic field. The coils were surrounded by an 18 mm inner-diameter container filled with FC-43. The hardware additions to the standard spectrometer consist of a four-way power splitter which is placed between the transmitter and the coils, and four radio frequency switches, shown in Fig. 7. The position of the switch is controlled by one of the five TTL outputs from the spectrometer. The four outputs of the switches are connected to the four receiver channels, each of which consists of an independent preamplifier, transmit/receive switch and analog-to-digital converter. The timing diagram describing the pulse sequence and data acquisition scheme is also shown in Fig. 7.

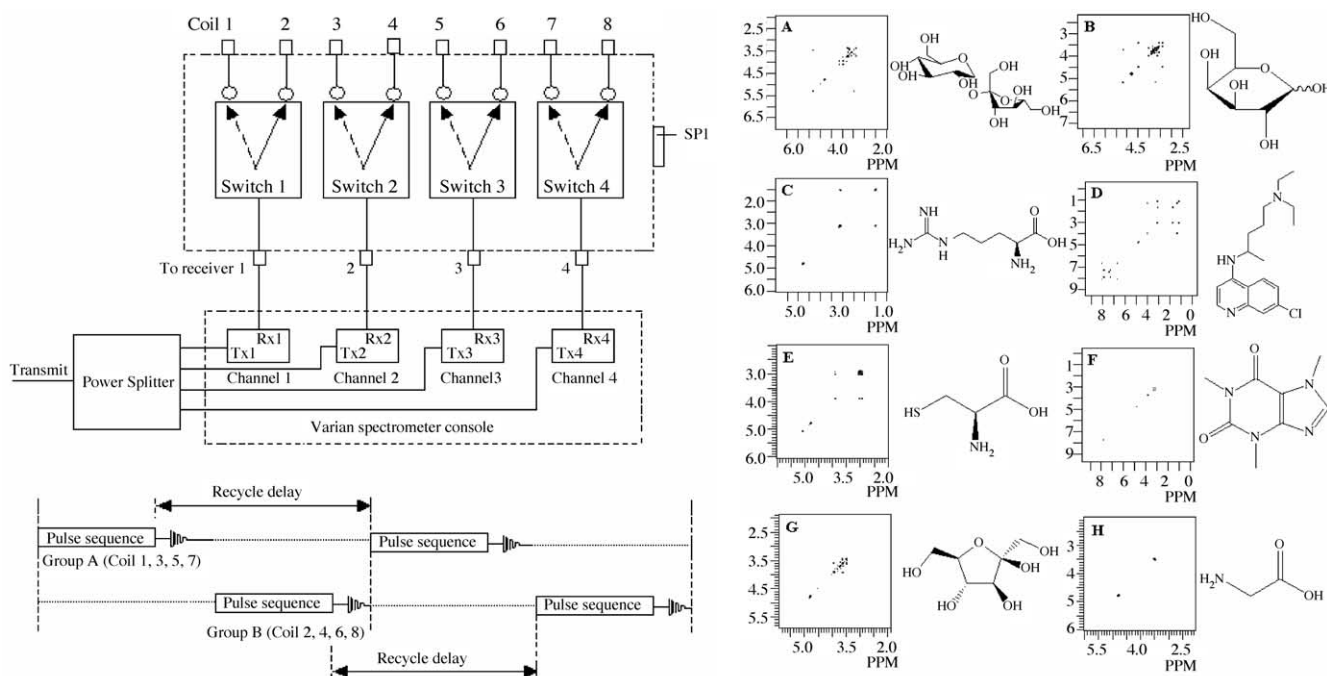


Fig. 7. (Top left) Schematic showing the full transmit and receive scheme. The four switching networks were controlled by TTL signals from the Varian Unity console. The eight coils were divided into two groups, A (coils 1, 3, 5, 7) and B (coils 2, 4, 6, 8). (Bottom left) Timing diagram showing the pulse sequence and data acquisition scheme used. (Right) COSY spectra acquired with the eight-coil probe and the chemical structures of the compounds used. Each sample (10 mM solution in  $D_2O$ ) was loaded into the coil via the attached Teflon tubes. (A) Sucrose, (B) galactose, (C) arginine, (D) chloroquine, (E) cysteine, (F) caffeine, (G) fructose and (H) glycine. Data acquisition parameters: data matrix  $2048 \times 256$ , eight scans,  $sw = 6000$  Hz and  $sw_1 = 6000$  Hz. Data were zero filled in  $t_1$  to 2048 points, processed with shifted sine-bell window functions applied in both dimensions, symmetrized and displayed in magnitude mode. Figure reproduced from Ref. [63], © 2004 with permission from Elsevier.

Since the spectrometer has only four receiver channels, the eight coils were divided into two groups, each containing four coils. The RF pulse sequence was transmitted to, and data acquired from, one coil group at a time. With a “compromise” value of the shim currents the linewidths for all eight coils were between 3 and 6 Hz. Two-dimensional COSY, TOCSY and gradient COSY experiments were run on eight different samples at 600 MHz. Fig. 7 shows the results from the COSY experiments.

A key component in increasing NMR throughput is integration with multiple separation columns or fluidic devices, which can load multiple samples in a reproducible fashion. In a recent paper, Macnaughtan et al. [61] showed that a four-coil “Multiplex probe” consisting of four solenoidal coils connected in parallel could be interfaced with a robotics liquid sampler and 96-well plate. Simultaneous injection of four compounds allowed an analysis rate of 34 s per sample for single scan one-dimensional proton spectroscopy. In this setup, plugs of  $D_2O$  separated by air bubbles were introduced around the samples, which were transferred to the probe via  $320 \mu\text{m}$  i.d. fused silica capillaries:  $35 \mu\text{L}$  of  $D_2O$  was injected, followed by  $25 \mu\text{L}$  of sample, a further  $35 \mu\text{L}$  of  $D_2O$  and  $15 \mu\text{L}$  of air,  $125 \mu\text{L}$  of  $H_2O$  was then used to push the samples into the centre of each of the coils of the Multiplex probe. Spectra were collected at 300 MHz with a

selective excitation sequence following water presaturation. The linewidths in each spectrum were between 1 and 2 Hz, and the metabolite concentrations used were 100 mM. Fig. 8 shows the physical setup of the system, and two sets of four spectra acquired using the probe.

In terms of extending multiple coil probeheads for applications such as protein/ligand binding or protein structure studies, multi-frequency coils must be designed with high isolation between all the resonant frequencies of all of the coils. One such probe, capable of acquiring two simultaneous  $^1H$ - $^{15}N$  HSQC spectra, has been designed for operation at 500 MHz, with two 3.5 mm long coils wrapped on a 2.6 mm o.d. polyimide sheath: a glass tube of 2.5 mm o.d., 2.2 mm i.d. containing the protein sample can be slid into each polyimide sheath. Each of the two coils was double-tuned to  $^1H$  and  $^{15}N$  frequencies, and an external lock coil was incorporated to compensate for field drift: this lock coil consisted of a three-turn solenoid with outer diameter 1 mm and contained a capillary of  $D_2O$ , and was placed approximately 5 mm from the two detection solenoidal coils. The two sample coils were situated 6 mm apart, separated by a thin copper shield for increased electrical isolation (Fig. 9). Electrical measurements showed that there was negligible crosstalk ( $<-40$  dB) between sample coils at all frequencies. FC-43 was used for magnetic susceptibility matching in order to improve sam-



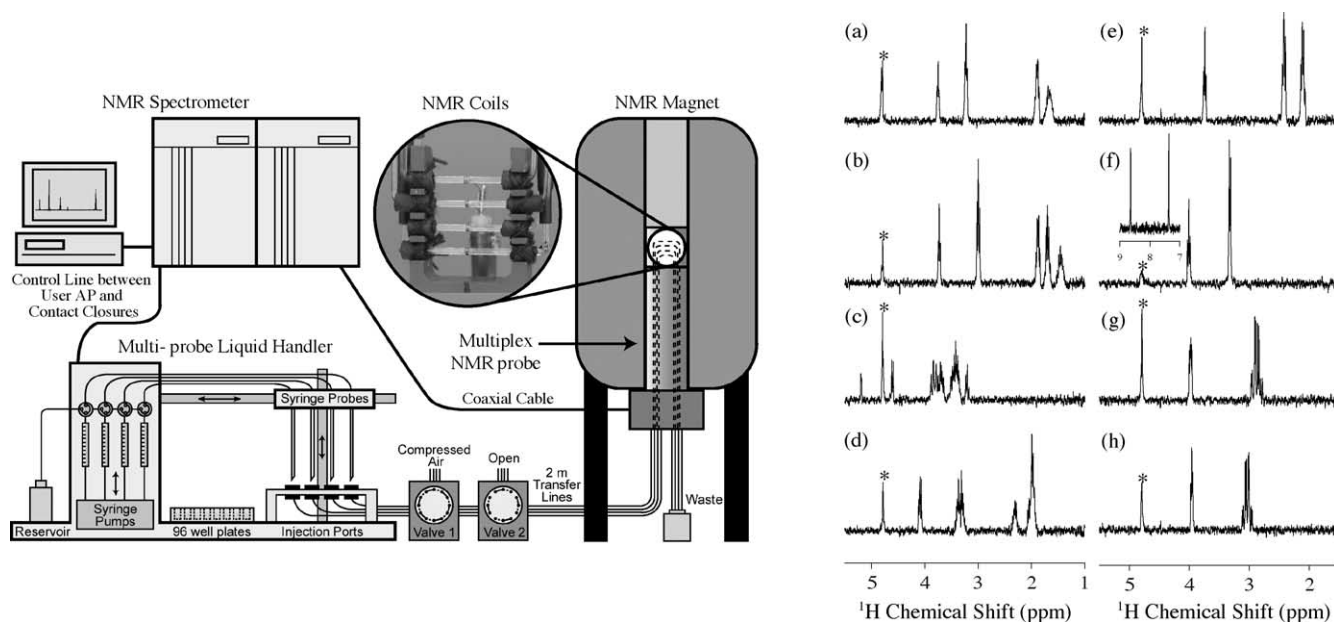


Fig. 8. (Left) The automation system includes a multiprobe liquid handler, two 12-port valves, the Multiplex NMR probe, and the NMR spectrometer. The liquid handler and spectrometer are electrically connected and communicate through the contact ports on the liquid handler and the user analog port on the spectrometer. The 12-port valves are controlled by the liquid handler and are used to control and remove the samples during the automation routine. The liquid handler can inject four samples at a time into the Multiplex probe through four transfer lines. The Multiplex flow probe, which is placed inside an NMR magnet, has four sample capillaries each with an NMR excitation/detection coil as shown in the photograph. (Right) Spectra of eight samples automatically injected into the Multiplex NMR probe were acquired with the automated flow injection routine: (a) L-arginine, (b) L-lysine, (c) D-(+)-glucose, (d) L-proline, (e) L-glutamine, (f) L-histidine, (g) L-asparagine, and (h) L-cysteine, all at 100 mM. The asterisks (\*) indicate the residual HDO peaks after suppression with a presaturation pulse. Reproduced with permission from Ref. [61], © 2003 American Chemical Society.

ple shimming. Two low-loss single-pole-five-throw (SP5T) switches are used to multiplex the signal into a single receiver.

In order to demonstrate the operation of this probe two proteins with widely different chemical shifts were used. This was most easily realized by using one protein which is unfolded (characterized by poorly dispersed chemical shifts and often having several high intensity narrow peaks from overlapping resonances) and one which is folded (usually characterized by a large chemical shift dispersion). The first coil was loaded with 1.25 mM  $^{15}\text{N}$ -labeled ubiquitin (VLI, Malvern, PA) in 90%  $\text{H}_2\text{O}/10\%$   $\text{D}_2\text{O}$  and 50 mM phosphate buffer at a pH of 5.5, and the second coil was loaded with 1 mM  $^{15}\text{N}$ -labeled IA-3 in 90%  $\text{H}_2\text{O}/10\%$   $\text{D}_2\text{O}$ , 50 mM phosphate buffer, also at a pH of 5.5.

Shimming was performed on the water free induction decay for each coil, using a low tip angle to avoid radiation damping, and gave linewidths of the water peaks for each sample of  $\sim 20$  Hz (a value that was very similar to that of either sample in a 5 mm commercial probehead). Fig. 9 shows two  $^1\text{H}-^{15}\text{N}$ HSQC spectra of the two proteins collected at the same time. The Varian spectrometer had only a single receiver channel, so data collection was staggered: pulse transmission and data acquisition for one sample were performed during the relaxation delay of the other sample. This relaxation delay was used for 1-s presaturation of the water signal using a shaped RF pulse. Immediately following data acquisition from the first coil, the two transmit/receive switches were shifted automatically to the second coil, and vice versa.

## 8. Hyphenation of microseparation techniques with NMR detection

The small detection volumes associated with NMR microcoils make it a natural choice for coupling with many chemical microseparation techniques such as capillary liquid chromatography [30,71–74], capillary electrophoresis and capillary electrochromatography [75–84] and capillary isotachopheresis [85–88]. In general, microseparation techniques enable faster analysis, higher concentration elution peaks and less chromatographic dilution than their larger scale counterparts. Since a number of review articles on this specific topic have been published recently [89–91], and coupled capillary HPLC–NMR forms the subject of another article in this issue, a detailed discussion is not included here. As in the case of “static” NMR, the use of small coils is ideally suited to small total sample amounts, present as relatively high concentrations in small volumes. As such, this often represents a trade-off between chromatographic resolution and NMR sensitivity, since the microcolumns may have to be overloaded. This also is an issue if one is trying to detect impurities at very low levels.

## 9. Other applications of small coils

Although outside the scope of this review article, the high intrinsic sensitivity of small NMR coils, and the ability to

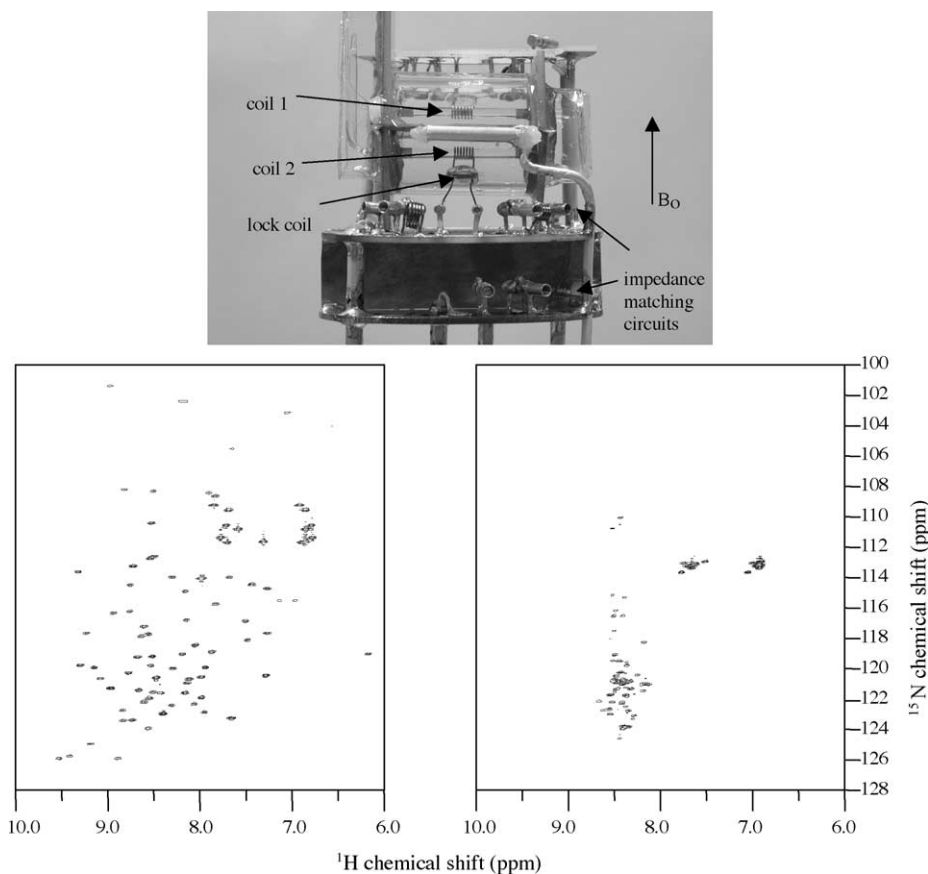


Fig. 9. (Top) A photograph of the two-coil probe assembly, together with the lock coil and impedance matching circuits. The samples are slid horizontally into the thin clear tubes around which the coils are formed. (Bottom left) A  $^1\text{H}$ - $^{15}\text{N}$  HSQC spectrum of 1.25 mM  $^{15}\text{N}$ -labeled ubiquitin in 90%  $\text{H}_2\text{O}/10\%$   $\text{D}_2\text{O}$ , 50 mM phosphate buffer, pH 5.5. Data acquisition parameters:  $\text{sw} = 4000$  Hz,  $\text{sw}1 = 1600$  Hz, 1024 complex data points, 192  $t_1$  increments acquired in States mode, 1 s water presaturation and 32 signal averages. Total data acquisition time 3.5 h. (Bottom right) A  $^1\text{H}$ - $^{15}\text{N}$  HSQC spectrum of 1 mM  $^{15}\text{N}$ -labeled IA-3 in 90%  $\text{H}_2\text{O}/10\%$   $\text{D}_2\text{O}$ , 50 mM phosphate buffer, pH 5.5. Identical data acquisition parameters were used. Data were acquired in interleaved fashion with pulse transmission and data reception routed through an RF switch controlled from the console.

study very small samples, has been exploited in many other areas of magnetic resonance. For example, magnetic resonance imaging and localized spectroscopy experiments have been performed on single neurons [92,93], and probeheads with multiple coils have also been used for cellular studies [94]. The strong  $B_1$  field produced by small coils has been exploited to cover the very large bandwidths required for certain solid-state applications [95]. Finally, multinuclear studies of small crystals have also recently been presented [96] using designs in which the goniometer is moved outside the RF coil, enabling much higher filling factors and S/N to be achieved than previously possible.

## 10. Conclusion

After initial work in the 1970s, the past decade has seen a rapid expansion in small coil development for high-resolution NMR spectroscopy. Higher  $B_0$  fields, cryogenic probe technology and “microcoils” have enabled successful realization of a number of NMR applications, which were previously not

possible due to low S/N. With comparable mass sensitivities, microprobes and cryoprobes play complementary roles in NMR studies: the facility of microprobe use is advantageous in applications where relatively high concentrations are possible, whereas cryogenic probes come into their own where lower concentrations are necessary. The relatively new area of multiple coil probehead shows great promise, not only in enabling high throughput NMR to become a practical reality, but also in enabling completely new types of experiment to be performed.

## Acknowledgements

This work was supported in part by the National Institutes of Health (EB002343), the National Science Foundation (DBI 97-22320) and the Alexander von Humboldt Foundation (Wolfgang Paul Preis). The author is grateful to Drs. Wolfgang Peti, Klaus Albert, Arthur Edison and Daniel Raftery for providing figures.

## References

- [1] R.F. Service, *Science* 279 (1998) 1127–1128.
- [2] P. Styles, N.F. Soffe, C.A. Scott, D.A. Cragg, F. Row, D.J. White, P.C.J. White, *J. Magn. Reson.* 60 (1984) 397–404.
- [3] C.R. Bowers, D.P. Weitekamp, *Phys. Rev. Lett.* 57 (1986) 2645–2648.
- [4] J.H. Ardenkjaer-Larsen, B. Fridlund, A. Gram, G. Hansson, L. Hansson, M.H. Lerche, R. Servin, M. Thaning, K. Golman, *Proc. Natl. Acad. Sci. U.S.A.* 100 (2003) 10158–10163.
- [5] W. Peti, J. Norcross, G. Eldridge, M. O'Neil-Johnson, *J. Am. Chem. Soc.* 126 (2004) 5873–5878.
- [6] V. Thomsen, D. Schatzlein, D. Mercurio, *Spectroscopy* 18 (2003) 112–114.
- [7] IUPAC Compendium of Chemical Terminology, second ed., 1997.
- [8] D.I. Hoult, R.E. Richards, *J. Magn. Reson.* 24 (1976) 71–85.
- [9] Y. Lin, S. Ahn, N. Murali, W. Brey, C.R. Bowers, W.S. Warren, *Phys. Rev. Lett.* 85 (2000) 3732–3735.
- [10] J. Haase, F. Steglich, D. Eckert, H. Siegel, H. Eschrig, K.H. Muller, *Solid State Nucl. Magn. Reson.* 23 (2003) 263–265.
- [11] M. Jerosch-Herold, R.K. Kirschman, *J. Magn. Reson.* 85 (1989) 141–146.
- [12] W.H. Wong, R.S. Withers, R. Nast, V.Y. Kotsubo, M.E. Johansson, H.D.W. Hill, L.F. Fuks, K.A. Kelin, B. Cole, W.W. Brey, A. Barfknecht, W.A. Anderson, *Adv. Cryog. Eng.* 42 (1996) 953–959.
- [13] N. Murali, G. Wang, C. Jolivet, T.M. Logan, *Magn. Reson. Chem.* 37 (1999) 512–515.
- [14] D.J. Russell, C.E. Hadden, G.E. Martin, A.A. Gibson, A.P. Zens, J.L. Carolan, *J. Nat. Prod.* 63 (2000) 1047–1049.
- [15] R.C. Crouch, W. Llanos, G. Knut, C.E. Hadden, D.J. Russell, G.E. Martin, *Magn. Reson. Chem.* 39 (2001) 555–558.
- [16] J.L. Griffin, H. Keun, C. Richter, D. Moskau, C. Rae, J.K. Nicholson, *Neurochem. Int.* 42 (2003) 93–99.
- [17] T.L. Peck, R.L. Magin, P.C. Lauterbur, *J. Magn. Reson. Ser. B* 108 (1995) 114–124.
- [18] J.N. Shoolery, *Top. Carbon-13 NMR Spectrosc.* 3 (1979) 28–38.
- [19] R.C. Crouch, G.E. Martin, *J. Nat. Prod.* 55 (1992) 1343–1347.
- [20] G.E. Martin, R.C. Crouch, *Magn. Reson. Chem.* 37 (1999) 721–729.
- [21] G. Schlotterbeck, A. Ross, R. Hochstrasser, H. Senn, T. Kuhn, D. Marek, O. Schett, *Anal. Chem.* 74 (2002) 4464–4471.
- [22] T. Barbara, *J. Magn. Reson. Ser. A* 109 (1994) 265–269.
- [23] W.L. Fitch, G. Detre, C.P. Holmes, J.N. Shoolery, P.A. Keifer, *J. Org. Chem.* 59 (1994) 7955–7956.
- [24] D.L. Olson, T.L. Peck, A.G. Webb, R.L. Magin, J.V. Sweedler, *Science* 270 (1995) 1967–1970.
- [25] A.G. Webb, S.C. Grant, *J. Magn. Reson.* 113 (1996) 83–87.
- [26] R. Subramanian, A.G. Webb, *Anal. Chem.* 70 (1998) 2454–2458.
- [27] R. Subramanian, M. Lam, A.G. Webb, *J. Magn. Reson.* 133 (1998) 227–231.
- [28] M.E. Lacey, R. Subramanian, D.L. Olson, A.G. Webb, J.V. Sweedler, *Chem. Rev.* 99 (1999) 3133–3152.
- [29] R. Subramanian, J.V. Sweedler, A.G. Webb, *J. Am. Chem. Soc.* 121 (1999) 2333–2334.
- [30] M. Krucker, A. Lienau, K. Putzbach, M.D. Grynbau, P. Schuler, K. Albert, *Anal. Chem.* 76 (2004) 2623–2628.
- [31] A.G. Webb, *NMR Spectrosc.* 31 (1997) 1–42.
- [32] F. Engelke, *Magn. Reson. Eng.* 15 (2002) 129–155.
- [33] P.F. Ryff, *IEEE Trans. Indus. App.* IA-8 (1972) 485–490.
- [34] K.R. Minard, R.A. Wind, *Concepts Magn. Reson.* 13 (2001) 128–142.
- [35] K.R. Minard, R.A. Wind, *Concepts Magn. Reson.* 13 (2001) 190–210.
- [36] S. Idziak, U. Haeberlen, *J. Magn. Reson.* 50 (1982) 281–288.
- [37] J.E. Stocker, T.L. Peck, A.G. Webb, M. Feng, R.L. Magin, *IEEE Trans. Biomed. Eng.* 44 (1997) 1122–1127.
- [38] J.A. Rogers, R.J. Jackman, G.M. Whitesides, D.L. Olson, J.V. Sweedler, *App. Phys. Lett.* 70 (1997) 2464–2466.
- [39] J. Dechow, T.E. Lanz, M. Stumber, A. Forchel, A. Haase, *Microelectron. Eng.* 53 (2000) 517–519.
- [40] J.D. Trumbull, I.K. Glasgow, D.J. Beebe, R.L. Magin, *IEEE Trans. Biomed. Eng.* 47 (2000) 3–7.
- [41] C. Massin, G. Boero, F. Vincent, J. Abenheim, P.-A. Besse, R.S. Popovic, *Sens. Actuators A* 97–98 (2002) 280–288.
- [42] C. Massin, F. Vincent, A. Homsy, K. Ehrmann, G. Boero, P.A. Besse, A. Daridon, E. Verpoorte, N.F. de Rooij, R.S. Popovic, *J. Magn. Reson.* 164 (2003) 242–255.
- [43] J.H. Walton, J.S. de Ropp, M.V. Shutov, A.G. Goloshevsky, M.J. McCarthy, R.L. Smith, S.D. Collins, *Anal. Chem.* 75 (2003) 5030–5036.
- [44] B. Sorli, J.F. Chateaux, M. Pitaval, H. Chahboune, B. Favre, A. Briguet, P. Morin, *Meas. Sci. Technol.* 15 (2004) 877–880.
- [45] Y. Maguire, R. Elavarasan, I.L. Chuang, N. Gershenfeld, *Experimental NMR Conference, Asilomar, CA, 2004.*
- [46] D.L. Olson, J.A. Norcross, M. O'Neil-Johnson, P.F. Molitor, D.J. Detlefsen, A.G. Wilson, T.L. Peck, *Anal. Chem.* 76 (2004) 2966–2974.
- [47] M.E. Lacey, J.V. Sweedler, C.K. Larive, A.J. Pipe, R.D. Farrant, *J. Magn. Reson.* 153 (2001) 215–222.
- [48] J.L. Griffin, A.W. Nicholls, H.C. Keun, R.J. Mortishire-Smith, J.K. Nicholson, T. Kuehn, *Analyst* 127 (2002) 582–585.
- [49] G.R. Eldridge, H.C. Vervoort, C.M. Lee, P.A. Cremin, C.T. Williams, S.M. Hart, M.G. Goering, M. O'Neil-Johnson, L. Zeng, *Anal. Chem.* 74 (2002) 3963–3971.
- [50] Y. Nakayama, K. Senokuchi, K. Sakaki, M. Kato, T. Maruyama, T. Miyazaki, H. Ito, H. Nakai, M. Kawamura, *Bioorg. Med. Chem.* 5 (1997) 971–985.
- [51] Y. Li, T. Logan, A. Edison, A.G. Webb, *J. Magn. Reson.* 164 (2003) 128–135.
- [52] M. Li, L.H. Phylip, W.E. Lees, J.R. Winther, B.M. Dunn, A. Wlodawer, J. Kay, A. Gustchina, *Nat. Struct. Biol.* 7 (2000) 113–117.
- [53] W. Peti, T. Etezady-Esfarjani, T. Herrmann, H.E. Klock, S.A. Lesley, K. Wuthrich, *J. Struct. Funct. Genomics* 5 (2004) 205–215.
- [54] L.E. Kay, G.-Y. Xu, A.U. Singer, D.R. Muhandiram, J.D. Forman-Kay, *J. Magn. Reson. Ser. B* 101 (1993) 333–337.
- [55] W. Peti, C. Griesinger, W. Bermel, *J. Biomol. NMR* 18 (2000) 199–205.
- [56] G. Fisher, C. Pettuci, E. MacNamara, D. Raftery, *J. Magn. Reson.* 138 (1999) 160–163.
- [57] Y. Li, A. Wolters, P. Malaway, J.V. Sweedler, A.G. Webb, *Anal. Chem.* 71 (1999) 4815–4820.
- [58] E. MacNamara, T. Hou, G. Fisher, S. Williams, D. Raftery, *Anal. Chim. Acta* 397 (1999) 9–16.
- [59] T. Hou, J. Smith, E. MacNamara, M. Macnaughtan, D. Raftery, *Anal. Chem.* 73 (2001) 2541–2546.
- [60] X. Zhang, J.V. Sweedler, A.G. Webb, *J. Magn. Reson.* 153 (2001) 254–258.
- [61] M.A. Macnaughtan, T. Hou, J. Xu, D. Raftery, *Anal. Chem.* 75 (2003) 5116–5123.
- [62] D. Raftery, *Anal. Bioanal. Chem.* 378 (2004) 1403–1404.
- [63] H. Wang, L. Ciobanu, A.S. Edison, A.G. Webb, *J. Magn. Reson.* 170 (2004) 206–212.
- [64] A.M. Wolters, D.A. Jayawickrama, A.G. Webb, J.V. Sweedler, *Anal. Chem.* 74 (2002) 5550–5555.
- [65] L. Ciobanu, D.A. Jayawickrama, X. Zhang, A.G. Webb, J.V. Sweedler, *Angew. Chem. Int. Ed. Engl.* 42 (2003) 4669–4672.
- [66] M.A. Macnaughtan, T. Hou, E. MacNamara, R. Santini, D. Raftery, *J. Magn. Reson.* 156 (2002) 97–103.
- [67] P.J. Hajduk, T. Gerfin, J.M. Boehlen, M. Haberli, D. Marek, S.W. Fesik, *J. Med. Chem.* 42 (1999) 2315–2317.
- [68] B.J. Stockman, K.A. Farley, D.T. Angwin, *Methods Enzymol.* 338 (2001) 230–246.
- [69] C. Dalvit, P.E. Fagerness, D.T. Hadden, R.W. Sarver, B.J. Stockman, *J. Am. Chem. Soc.* 125 (2003) 7696–7703.

- [70] C. Dalvit, D.T. Hadden, R.W. Sarver, A.M. Ho, B.J. Stockman, *Comb. Chem. High Throughput Screen.* 6 (2003) 445–453.
- [71] B. Behnke, G. Schlotterbeck, U. Tallarek, S. Strohschein, L.-H. Tseng, T. Keller, K. Albert, E. Bayer, *Anal. Chem.* 68 (1996) 1110–1115.
- [72] K. Albert, G. Schlotterbeck, L.-H. Tseng, U. Braumann, *J. Chromatogr. A* 750 (1996) 303–309.
- [73] R. Subramanian, W. Kelley, J. Tan, J.V. Sweedler, A.G. Webb, *Anal. Chem.* 71 (1999) 5335–5339.
- [74] M.E. Lacey, Z.J. Tan, A.G. Webb, J.V. Sweedler, *J. Chromatogr. A* 922 (2001) 139–149.
- [75] N. Wu, T.L. Peck, A.G. Webb, R.L. Magin, J.V. Sweedler, *J. Am. Chem. Soc.* 116 (1994) 7929–7930.
- [76] K. Pusecker, J. Schewitz, P. Gfrorer, L.-H. Tseng, K. Albert, E. Bayer, *Anal. Chem.* 70 (1998) 3280–3285.
- [77] J. Schewitz, P. Gfrorer, K. Pusecker, L.-H. Tseng, K. Albert, E. Bayer, I.D. Wilson, N.J. Bailey, G.B. Scarfe, J.K. Nicholson, *Analyst* 123 (1998) 2835–2837.
- [78] K. Pusecker, J. Schewitz, P. Gfrorer, L.-H. Tseng, K. Albert, E. Bayer, I.D. Wilson, N.J. Bailey, G.B. Scarfe, J.K. Nicholson, *Anal. Commun.* 35 (1998) 213–215.
- [79] D.L. Olson, M.E. Lacey, A.G. Webb, J.V. Sweedler, *Anal. Chem.* 71 (1999) 3070–3076.
- [80] J. Schewitz, K. Pusecker, P. Gfrorer, U. Gotz, L.-H. Tseng, K. Albert, E. Bayer, *Chromatographia* 50 (1999) 333–337.
- [81] P. Gfrorer, J. Schewitz, K. Pusecker, L.-H. Tseng, K. Albert, E. Bayer, *Electrophoresis* 20 (1999) 3–8.
- [82] P. Gfrorer, L.-H. Tseng, E. Rapp, K. Albert, E. Bayer, *Anal. Chem.* 73 (2001) 3234–3239.
- [83] M.E. Lacey, A.G. Webb, J.V. Sweedler, *Anal. Chem.* 74 (2002) 583–587.
- [84] M.E. Lacey, A.G. Webb, J.V. Sweedler, *Anal. Chem.* 72 (2000) 4991–4998.
- [85] R.A. Kautz, M.E. Lacey, A.M. Wolters, F. Foret, A.G. Webb, B.L. Kargar, J.V. Sweedler, *J. Am. Chem. Soc.* 123 (2001) 3159–3160.
- [86] A.M. Wolters, D.A. Jayawickrama, C.K. Larive, J.V. Sweedler, *Anal. Chem.* 74 (2002) 4191–4197.
- [87] A.M. Wolters, D.A. Jayawickrama, C.K. Larive, J.V. Sweedler, *Anal. Chem.* 74 (2002) 2306–2313.
- [88] D.A. Jayawickrama, J.V. Sweedler, *Anal. Bioanal. Chem.* 378 (2004) 1528–1535.
- [89] L.A. Cardoza, V.K. Almeida, A. Carr, C.K. Larive, D.W. Graham, *Trends Anal. Chem.* 22 (2003) 766–775.
- [90] P. Gfrorer, J. Schewitz, K. Pusecker, E. Bayer, *Anal. Chem.* 71 (1999) 315A–321A.
- [91] D.A. Jayawickrama, J.V. Sweedler, *J. Chromatogr. A* 1000 (2003) 819–840.
- [92] S.C. Grant, N. Aiken, T. Mareci, D. Plant, A.G. Webb, S. Blackband, *Magn. Reson. Med.* 44 (2000) 19–22.
- [93] S.C. Grant, D.L. Buckley, S. Gibbs, A.G. Webb, S.J. Blackband, *Magn. Reson. Med.* 46 (2001) 1107–1112.
- [94] A. Porea, T. Neuberger, A.G. Webb, *Magn. Reson. Eng.* 22B (2004) 7–14.
- [95] K. Yamauchi, J.W. Janssen, A.P. Kentgens, *J. Magn. Reson.* 167 (2004) 87–96.
- [96] T. Vosegaard, P. Daugaard, E. Hald, H.J. Jakobsen, *J. Magn. Reson.* 142 (2000) 379–381.